Catalytic oxidation of methacrolein to methacrylic acid over silica-supported 11-molybdo-1-vanadophosphoric acid with different heteropolyacid loadings

Mitsuru Kanno [a], Toshiya Yasukawa [b], Wataru Ninomiya [b], Ken Ooyachi [b], Yuichi Kamiya [c,*]

[a] Graduate School of Environmental Science, Hokkaido University, Kita 10 Nishi 5, Sapporo 060-0810, Japan
[b] Corporate Research Laboratories, Mitsubishi Rayon Co., Ltd., 20-1, Miyuki-cho, Otake, Hiroshima 739-0693, Japan
[c] Research Faculty of Environmental Earth Science, Hokkaido University, Kita 10 Nishi 5, Sapporo 060-0810, Japan

ABSTRACT

Catalytic oxidation of methacrolein (MAL) to methacrylic acid (MAA) over SiO_2-supported $H_4PMo_{11}VO_{40}$ with different $H_4PMo_{11}VO_{40}$ loadings was investigated. $H_4PMo_{11}VO_{40}/SiO_2$ showed high activity in comparison with unsupported $H_4PMo_{11}VO_{40}$, and 3.3 mol% $H_4PMo_{11}VO_{40}/SiO_2$ (50 wt.% $H_4PMo_{11}VO_{40}$) had the highest activity, which was five-times larger than that of unsupported $H_4PMo_{11}VO_{40}$ due to high dispersion of $H_4PMo_{11}VO_{40}$ on SiO_2, as determined by temperature-programmed desorption of benzonitrile. On the other hand, the supported catalysts were less selective toward the formation of MAA. From X-ray diffraction and Raman spectroscopy, it was determined that $H_4PMo_{11}VO_{40}$ decomposed to form MoO_3 on SiO_2 during the catalytic reaction. Since SiO_2-supported MoO_3 and unsupported MoO_3 had only very low selectivity toward the formation of MAA in the oxidation of MAL, it was concluded that the formation of MoO_3 caused the decrease in the catalytic performance of the supported catalysts.

© 2010 Elsevier Inc. All rights reserved.

1. Introduction

Methacrylic acid (MAA) is an important intermediate in the production of methyl methacrylate and other derivatives, including polymers. Selective oxidation to produce MAA via methacrolein (MAL) is a two-stage process involving the oxidation of isobutene to MAL, followed by MAL to MAA. The first step of the reaction is conducted in the presence of a Mo–Bi-oxide catalyst, and the second step involves Keggin-type heteropoly compounds containing Mo, V, and P as catalysts [1,2]. The oxidation of MAL to MAA has some issues, and in order to improve the yield of MAA, a highly active and selective catalyst is needed.

Selective oxidation of MAL over heteropoly compounds composed of P and Mo has been studied extensively [3–14]. It has been shown that substituting some Mo atoms with V atoms improves the catalytic activity and selectivity for the formation of MAA [13]. In addition, substituting H^+ with Cs^+ retards the oxidation of MAA to CO and CO_2 [13,14].

Solid heteropolyacids, that is to say, unsupported heteropolyacids, can be used as heterogeneous catalysts. However, they have low surface area and consequently have only a small number of active sites available. Thus, solid heteropolyacids frequently show only low catalytic activity. Increasing the surface area of heteropolyacids by supporting them on a carrier with a high surface area could

afford highly active catalysts. Supporting $H_3PW_{12}O_{40}$ and $H_4SiW_{12}O_{40}$ on SiO_2, TiO_2, and active carbon shows a great success in solid acid catalysts [15–20]. As for oxidation catalysts, supported $H_{3+x}PMo_{12−x}V_xO_{40}$ ($x = 0–2$) have been investigated for gas-phase oxidations of methanol [21–24], ethanol [25,26], ethene [27], propene [28], ethane [29], isobutane [30], ammoxidation of 2-methyl pyrazine [31], and liquid-phase oxidations of tetrahydrothiophene [32,33], cycloalkenes [34], toluene [35], benzyl alcohol [36] and stylene [37,38]. Nowińska et al. have demonstrated that SiO_2-supported $H_5PMo_{10}V_2O_{40}$ is highly active than unsupported one for the oxidation of ethane [27]. Liu and Iglesia have reported that supporting $H_{3+n}PMo_{12−n}V_nO_{40}$ on SiO_2 enhances the catalytic activity and decreases the CO_x selectivity in a one-step synthesis of dimethoxymethane via the oxidation of dimethyl ether or methanol [21]. Kim et al. have reported that $H_3PMo_{12}O_{40}$ supported on a mesostructured cellular SiO_2 foam, in which the support has been modified with 3-aminopropyl triethoxysilane, shows high activity for the oxidation of ethanol to acetaldehyde at 503 K [25]. However, there are only a few reports on supported heteropolyacid catalysts being used in the selective oxidation of MAL. Kim et al. [39,40] have demonstrated that $H_5PMo_{10}V_2O_{40}$ supported on nitrogen-containing mesoporous carbon and $H_3PMo_{12}O_{40}$ supported on polystyrene have higher activity for the oxidation of MAL and selectivity toward the formation of MAA compared with the corresponding unsupported catalysts.

In this study, we investigated the catalytic performance of SiO_2-supported $H_4PMo_{11}VO_{40}$ for the selective oxidation of MAL to MAA

and compared its catalytic performance with unsupported $H_4PMo_{11}VO_{40}$. The effects of the loading amount of $H_4PMo_{11}VO_{40}$ on the activity and selectivity were investigated. Changes in the catalytic performance, especially selectivity against the loading amounts, are discussed in conjunction with the chemical and physical properties of the catalysts before and after the catalytic reaction.

2. Experimental

2.1. Preparation of catalysts

MoO$_3$, V$_2$O$_5$, and 85% H$_3$PO$_4$, which were used to prepare $H_4PMo_{11}VO_{40}$, were purchased from Wako Pure Chemical Co., Ltd. MoO$_3$ (31.7 g), V$_2$O$_5$ (1.82 g), and water (1.5 dm^3) were added to a roundbottom flask. After the addition of 85% H$_3$PO$_4$ (2.3 g) into the resulting suspension, it was heated and vigorously stirred at 358 K for 3 h. After the solution was cooled to room temperature, the insoluble matter was filtered off to obtain a clear orange solution. Then the solvent was evaporated to obtain $H_4PMo_{11}VO_{40}$, which was dried in air at 333 K overnight.

SiO$_2$-supported $H_4PMo_{11}VO_{40}$ with different $H_4PMo_{11}VO_{40}$ loadings were prepared by using an incipient-wetness method with an aqueous solution of $H_4PMo_{11}VO_{40}$ (0.08 mol dm^{-3}) and SiO$_2$ (Aerosil 300: 295 m^2 g^{-1}, Nippon Aerosil Co., Ltd.). $H_4PMo_{11}VO_{40}$/SiO$_2$ with 0.37, 1.4, and 3.3 mol% loadings, which correspond to 10, 30, and 50 wt.%, respectively, were prepared by changing the amount of the aqueous $H_4PMo_{11}VO_{40}$ solution added. The resulting wet solid was dried in air at 333 K overnight and was then calcined in air at 523 K for 4 h. Since each Keggin cluster (KU) occupies about 1.44 nm^2 [41], a theoretical monolayer of KU with 0.69 KU nm^{-2} formed. Thus, the catalysts with loadings of 0.37, 1.4, and 3.3 mol% correspond to monolayer coverages of 0.18, 0.71, and 1.65, respectively, if Keggin clusters are ideally dispersed on SiO$_2$.

As a reference, 3.96 mol% MoO$_3$/SiO$_2$ (9.0 wt.% MoO$_3$) was prepared by using an impregnation method involving SiO$_2$ and an aqueous solution of MoO$_3$, which was prepared by adding aqueous ammonia (25%, Wako Pure Chemical Co., Ltd.) to an aqueous suspension of MoO$_3$.

2.2. Characterization of catalysts

Powder X-ray diffraction (XRD) was performed using an X-ray diffractometer (Rigaku Mini Flex) with Cu Kα radiation (λ = 0.154 nm). Raman spectroscopy was performed using a laser Raman spectrometer (JASCO, RMP 200) with a 100-mW laser with a wavelength of 532 nm and a CCD detector. Temperature-programmed desorption of benzonitrile (BN-TPD) was carried out using a custom-built TPD system equipped with a mass spectrometer (ANELVA, M-QA100S) as a detector. After the catalyst was pretreated in a N$_2$ flow at 523 K for 1 h, it was exposed to 0.122 μmol h^{-1} of BN in a He flow at 373 K for 2 h. The weakly adsorbed or physisorbed BN was removed in a He flow at 373 K for 2 h and then at 393 K. The temperature was then increased at a rate of 10 K min^{-1} to 873 K under a He flow while monitoring the mass signals (m/e = 18, 28, 44, and 103 for H$_2$O, CO, CO$_2$, and BN, respectively) in the exit gas.

2.3. Catalytic reaction

Catalytic oxidation of MAL was performed in a continuous flow reactor at 573 K and atmospheric pressure. Before the reaction, the catalyst was pretreated under a flow of a gas mixture consisting of O$_2$ (10.7 vol.%), H$_2$O (17.9 vol.%), and N$_2$ (balance) at a total flow

rate of 28 cm^3 min^{-1} and a temperature of 593 K for 1 h. After the temperature was decreased to 573 K, a reactant gas mixture of MAL (3 vol.%), O$_2$ (6 vol.%), H$_2$O (15 vol.%), and N$_2$ (balance) was fed into the reactor to start the catalytic reaction. The amount of the catalyst and total flow rate were adjusted to control the conversion. The reaction products were analyzed by using on-line gas chromatographs (GCs) connected at the outlet of the reactor. For acetic acid (AcOH), MAL, and MAA, a GC (Shimadzu GC-14B) equipped with a flame ionization detector and a capillary column (TC-FFAP, 0.25 mm × 50 m) was utilized. For CO and CO$_2$, a GC (Shimadzu GC-8A) equipped with a thermal conductivity detector (TCD) and two packed columns (Molecular Sieve 5A, 2.85 mm × 3 m and Activated Carbon, 2.85 mm × 2 m) was used. In order to prevent interference from organic compounds, prior to the GC–TCD analysis, the gas was passed through a dry-ice trap to remove them. As an internal standard for GC analysis, CH$_4$ (31%) diluted with He was mixed at the outlet of the reactor.

3. Results and discussion

3.1. Catalytic oxidation of MAL over unsupported and SiO$_2$-supported $H_4PMo_{11}VO_{40}$

Fig. 1 shows time courses of the catalytic oxidation of MAL over unsupported $H_4PMo_{11}VO_{40}$ and 1.4 mol% $H_4PMo_{11}VO_{40}$/SiO$_2$, in which WF^{-1} were 101 and 17 g$_{-cat}$ h mol$_{-MAL}^{-1}$, respectively, where W is the weight of the catalyst (g) and F is the flow rate of MAL (mol h^{-1}). In the initial stage of the reaction, selectivity of unsupported $H_4PMo_{11}VO_{40}$ toward the formation of MAA slightly increased and then reached nearly constant values after 50 min. On the other hand, the conversion of MAL and the selectivity toward AcOH and CO$_x$ decreased with time in the initial stage of the reaction and reached nearly constant values after 50 min. For 1.4 mol% $H_4PMo_{11}VO_{40}$/SiO$_2$, although the selectivity changed in the initial stage of the reaction, constant selectivities were obtained within

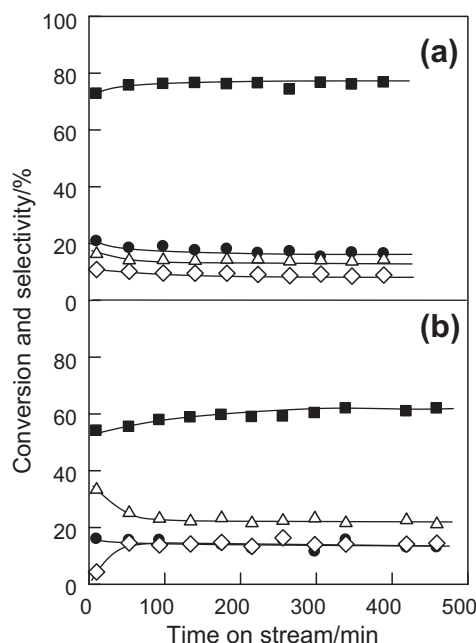**Fig. 1.** Time courses of oxidation of MAL over (a) unsupported $H_4PMo_{11}VO_{40}$ and (b) 1.4 mol% $H_4PMo_{11}VO_{40}$/SiO$_2$. (●) Conversion of MAL and selectivities for (■) methacrylic acid, (◇) acetic acid, and (△) CO$_x$. Reaction conditions: MAL:O$_2$: H$_2$O:N$_2$ = 3:6:15:76, temperature = 573 K, total pressure = 0.1 MPa, and WF^{-1} = 101 and 17 g$_{-cat}$ h mol$_{-MAL}^{-1}$ for unsupported $H_4PMo_{11}VO_{40}$ and 1.4 mol% $H_4PMo_{11}VO_{40}$/SiO$_2$, respectively.

300 min. Conversion of MAL was basically constant during the reaction. Since 0.37 and 3.3 mol% $H_4PMo_{11}VO_{40}/SiO_2$ also showed constant conversions and selectivities within 300 min, the activity and selectivities were estimated from data obtained after 300 min.

In Fig. 2, the catalytic activity and selectivity are plotted as a function of the loading amount of $H_4PMo_{11}VO_{40}$ on SiO_2, where catalytic activity means the rate of MAL consumed per total weight of the catalyst. Catalytic activities and selectivities were determined from data obtained at ~10% conversion. Unsupported $H_4PMo_{11}VO_{40}$ had a catalytic activity of 13 $\mu mol\,g^{-1}\,min^{-1}$ at 573 K, whereas 3.3 mol% $H_4PMo_{11}VO_{40}/SiO_2$ had a catalytic activity of 74 $\mu mol\,g^{-1}\,min^{-1}$, which is 5 times higher than that of unsupported $H_4PMo_{11}VO_{40}$. However, the catalytic activity decreased with a decrease in the loading amount, and 0.37 mol% $H_4PMo_{11}VO_{40}/SiO_2$ showed activity similar to that of unsupported $H_4PMo_{11}VO_{40}$. However, if we consider the amount of $H_4PMo_{11}VO_{40}$ contained in 0.37 mol% $H_4PMo_{11}VO_{40}/SiO_2$, the catalytic activity per unit weight of $H_4PMo_{11}VO_{40}$ is 10 times higher for 0.37 mol% $H_4PMo_{11}VO_{40}/SiO_2$ than it is for the unsupported catalyst. This improvement in the catalytic activity is due to the increase in the number of $H_4PMo_{11}VO_{40}$ exposed on the outermost surface by supporting it on SiO_2. This effect will be discussed in detail in Section 3.2.

In contrast to the catalytic activity, selectivities toward the formation of MAA of SiO_2-supported $H_4PMo_{11}VO_{40}$ were slightly lower than that of unsupported $H_4PMo_{11}VO_{40}$. Unsupported $H_4PMo_{11}VO_{40}$ showed 75% selectivity for the formation of MAA. The selectivities of 3.3 and 1.4 mol% $H_4PMo_{11}VO_{40}/SiO_2$ were 66% and 63%, respectively. However, 0.37 mol% $H_4PMo_{11}VO_{40}/SiO_2$ was much less selective.

3.2. Kinetic study on the oxidation of MAL over unsupported and SiO_2-supported $H_4PMo_{11}VO_{40}$

In order to investigate the effect of supporting $H_4PMo_{11}VO_{40}$ on SiO_2 on the oxidation of MAL, we used 1.4 mol% $H_4PMo_{11}VO_{40}/SiO_2$ as a typical supported catalyst and compared its catalytic properties with unsupported $H_4PMo_{11}VO_{40}$ via a kinetic study. Fig. 3 shows selectivity dependences on the conversion of MAL for
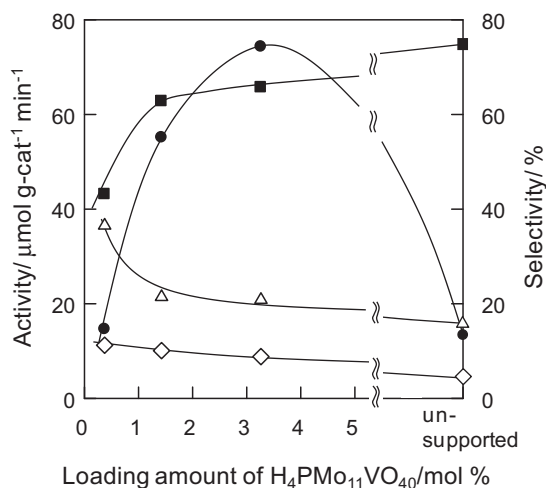

Fig. 2. Effects of the loading amount of $H_4PMo_{11}VO_{40}$ on SiO_2 on the catalytic activity and selectivity. (●) Activity and selectivities for (■) MAA, (◇) acetic acid, and (△) CO_x. Reaction conditions: $MAL:O_2:H_2O:N_2$ = 3:6:15:76, temperature = 573 K, pressure = 0.1 MPa, WF^{-1} = 99, 28, 29, and 75 $g_{-cat}\,h\,mol_{-MAL}^{-1}$ for unsupported $H_4PMo_{11}VO_{40}$, 3.3 mol% $H_4PMo_{11}VO_{40}/SiO_2$, 1.4 mol% $H_4PMo_{11}VO_{40}/SiO_2$, and 0.37 mol% $H_4PMo_{11}VO_{40}/SiO_2$, respectively. Activities were calculated from the data at the conversions in the range of 8–12%. Selectivities were evaluated using conversions in the range of 8–12%.
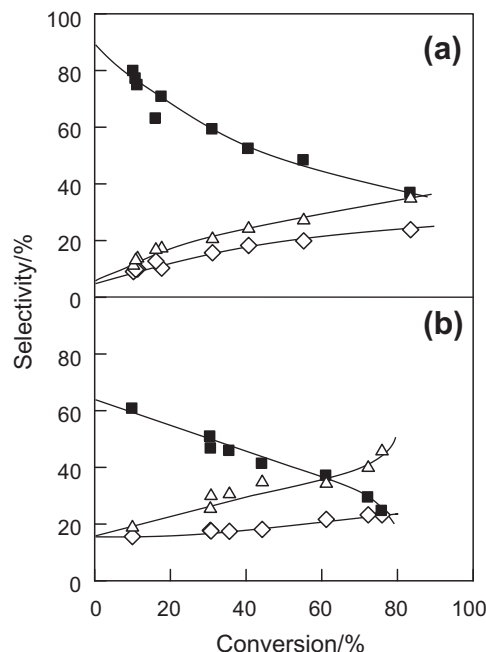

Fig. 3. Relationship between selectivity and conversion for (a) unsupported $H_4PMo_{11}VO_{40}$ and (b) 1.4 mol% $H_4PMo_{11}VO_{40}/SiO_2$. (■) MAA, (◇) acetic acid, and (△) CO_x. Reaction conditions: $MAL:O_2:H_2O:N_2$ = 3:6:15:76, temperature = 573 K, and total pressure = 0.1 MPa.

unsupported $H_4PMo_{11}VO_{40}$ and 1.4 mol% $H_4PMo_{11}VO_{40}/SiO_2$. At low conversion, the selectivity for MAA formation was relatively high for both catalysts, and the selectivities for AcOH and CO_x were low. However, the selectivity for MAA decreased as the conversion increased for both catalysts, indicating that MAA was successively oxidized to AcOH and CO_x. When the selectivity was extrapolated to 0% conversion, the selectivities of unsupported $H_4PMo_{11}VO_{40}$ for MAA, AcOH and CO_x were 84%, 7%, and 9%, respectively, and those of 1.4 mol% $H_4PMo_{11}VO_{40}/SiO_2$ were 65%, 15%, and 15%, respectively. It should be emphasized that the selectivities for AcOH and CO_x were not 0% even at 0% conversion for both catalysts, indicating that AcOH and CO_x directly form from MAL. Based on these findings, we propose the reaction pathway shown in Scheme 1.

We assumed that the reaction to consume MAL was a first-order reaction, where the first-order reaction rate constant (k_{total}) corresponds to the sum of each rate constant (k_1, k_2, and k_3 in Scheme 1). By optimizing k_{total}, the behavior of the WF^{-1} dependencies on the conversion of MAL could be fitted for both catalysts, and values of k_{total} were estimated to be $0.94 \times 10^{-3}\,h^{-1}\,g_{-cat}^{-1}$ and $3.5 \times 10^{-3}\,h^{-1}\,g_{-cat}^{-1}$ for unsupported $H_4PMo_{11}VO_{40}$ and 1.4 mol% $H_4PMo_{11}VO_{40}/SiO_2$, respectively. Thus, k_1, k_2, and k_3 for the conversion of MAL to MAA, AcOH, and CO_x, respectively, could be calculated from Eq. (1) by using the selectivity at 0% conversion. The values are summarized in Table 1.
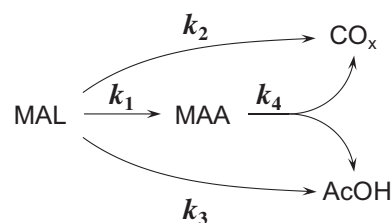
Scheme 1. Reaction pathway for the oxidation of MAL over $H_4PMo_{11}VO_{40}$ catalysts.

Table 1
First-order reaction rate constants for the oxidation of MAL over unsupported $H_4PMo_{11}VO_{40}$ and 1.4 mol% $H_4PMo_{11}VO_{40}/SiO_2$.

Catalyst	Reaction rate constant[a] $\left(\times 10^{-3} \text{ h}^{-1} \text{ g}_{-cat}^{-1}\right)$					k_4/k_1
	k_{total}	k_1	k_2	k_3	k_4	
$H_4PMo_{11}VO_{40}$	0.94	0.79	0.066	0.084	0.51	0.65
1.4 mol% $H_4PMo_{11}VO_{40}/SiO_2$	3.5 (3.7)[b]	2.3 (2.9)[b]	0.53 (8.0)[b]	0.53 (6.3)[b]	3.0 (5.9)[b]	1.3

[a] Reactions for the rate constants are shown in Scheme 1.
[b] Figures in parenthesis are relative rates for 1.4 mol% $H_4PMo_{11}VO_{40}/SiO_2$ against the corresponding reaction rates for unsupported $H_4PMo_{11}VO_{40}$.

$$k_n = k_{total} \times \frac{\text{Selectivity (\%) at 0\% conversion}}{100} \quad (n = 1, 2, 3) \quad (1)$$

In order to evaluate the influence of the support on successive oxidation reactions of MAA, we assumed that the reactions of MAA to AcOH and CO_x and MAL to MAA were first-order reactions. Thus, the yield of MAA could be determined as follows:

$$\text{Yield of MAA} = \frac{k_1}{-(k_1 + k_2 + k_3) + k_4} \times [\text{MAL}]_0 \times (e^{-(k_1+k_2+k_3)t} - e^{-k_4 t}) \quad (2)$$

where k_1, k_2, k_3, and k_4 are rate constants, $[\text{MAL}]_0$ is the concentration of MAA at the inlet of the reactor, and t is WF^{-1}. In Fig. 4, the yield of MAA is plotted as a function of WF^{-1}. The experimental yields were fitted in relation to k_1, k_2, k_3, and an optimized value of k_4 and are also shown in Fig. 4. k_4 and the ratio of k_4/k_1 for $H_4PMo_{11}VO_{40}$ and 1.4 mol% $H_4PMo_{11}VO_{40}/SiO_2$ are summarized in Table 1. It is noted that the k_4/k_1 ratio is two-times larger for 1.4 mol% $H_4PMo_{11}VO_{40}/SiO_2$ (=1.3) than it is for unsupported $H_4PMo_{11}VO_{40}$ (=0.65), indicating that the successive reaction of MAA, which results in a decrease of the maximum MAA yield, is accelerated more greatly over 1.4 mol% $H_4PMo_{11}VO_{40}/SiO_2$ than it is over unsupported $H_4PMo_{11}VO_{40}$. In summary, supporting $H_4PMo_{11}VO_{40}$ on SiO_2 promoted both selective and non-selective reactions; however, the non-selective reactions were accelerated to a great extent (Table 1).

3.3. Physical and chemical properties of catalysts

As mentioned earlier, supporting $H_4PMo_{11}VO_{40}$ on SiO_2 improved the catalytic activity but lowered selectivity for the formation of MAA. Thus, we next investigated the cause of the increase in the activity and the decrease in the selectivity by using physico-chemical characterization techniques.

3.3.1. Pre-catalytic oxidation of MAL
Fig. 5 shows XRD patterns of the catalysts before the reaction. The diffraction pattern of unsupported $H_4PMo_{11}VO_{40}$ (Fig. 5a) was identical to that of $H_4PMo_{11}VO_{40}\cdot14H_2O$ [42]. In the case of the supported catalysts, 3.3 mol% $H_4PMo_{11}VO_{40}/SiO_2$ had a diffraction pattern corresponding to $H_4PMo_{11}VO_{40}\cdot14H_2O$, but the intensities

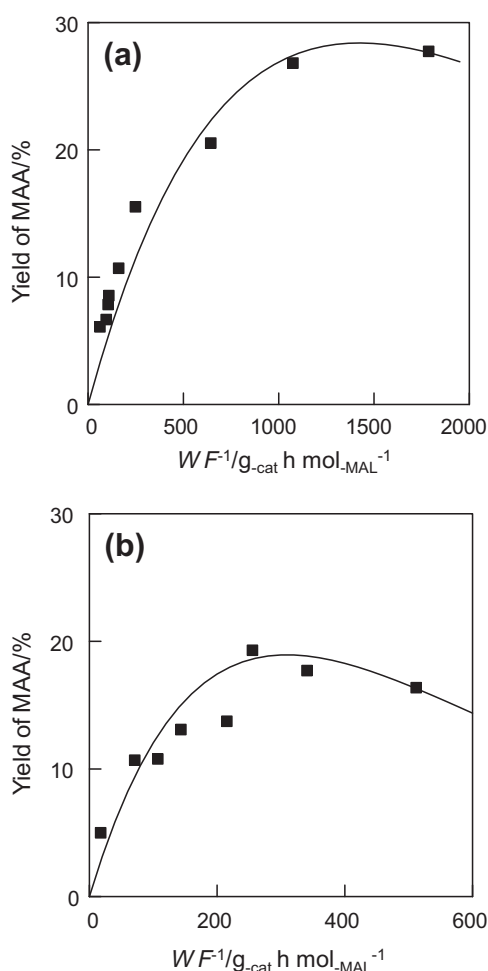**Fig. 4.** Experimental data (■) and yield of MAA calculated (–) using the optimized reaction rate constant k_4 for (a) Unsupported $H_4PMo_{11}VO_{40}$ and (b) 1.4 mol% $H_4PMo_{11}VO_{40}/SiO_2$. Reaction conditions: MAL:O$_2$:H$_2$O:N$_2$ = 3:6:15:76, temperature = 573 K, and total pressure = 0.1 MPa.
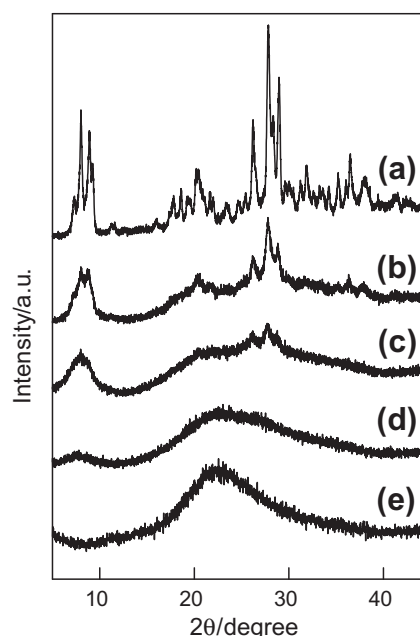

Fig. 5. XRD patterns of unsupported and SiO$_2$-supported $H_4PMo_{11}VO_{40}$ before the reaction. (a) Unsupported $H_4PMo_{11}VO_{40}$, SiO$_2$-supported $H_4PMo_{11}VO_{40}$ with loadings of (b) 3.3 mol%, (c) 1.4 mol%, (d) 0.37 mol% and (e) SiO$_2$.

of the diffraction lines were weaker than those of the unsupported catalyst. The intensities of the diffraction lines gradually decreased with a decrease in the loading amount, and in the case of 0.37 mol% $H_4PMo_{11}VO_{40}/SiO_2$, no diffraction lines for the crystalline heteropolyacid were observed. Since even a physical mixture of unsupported $H_4PMo_{11}VO_{40}$ (0.37 mol%) and SiO_2 (99.63 mol%) showed a clear diffraction pattern due to $H_4PMo_{11}VO_{40} \cdot 14H_2O$ (data not shown), $H_4PMo_{11}VO_{40}$ was highly dispersed on the SiO_2 in the supported catalysts.

Fig. 6 shows Raman spectra of the catalysts before the reaction. In the spectrum for unsupported $H_4PMo_{11}VO_{40}$ (Fig. 6a), only the four characteristic bands of a Keggin structure were observed: 1000, 907, 624, and 242 cm^{-1} for $\nu_s(Mo–O_t)$, $\nu_s(Mo–O_b–Mo)$, $\nu_s(Mo–O_c–Mo)$, and $\nu_s(Mo–O_a)$, respectively [43]. 1.4 and 3.3 mol% $H_4PMo_{11}VO_{40}/SiO_2$ showed Raman bands corresponding to $H_4PMo_{11}VO_{40}$, indicating that at least some $H_4PMo_{11}VO_{40}$ was retained. It should be emphasized that Raman bands due to $H_4PMo_{11}VO_{40}$ for the supported catalysts shifted toward lower wave numbers with a decrease in the loading amount of $H_4PMo_{11}VO_{40}$. For example, $\nu_s(Mo–O_c–Mo)$ was observed at 907 cm^{-1} for unsupported $H_4PMo_{11}VO_{40}$, whereas it was observed at 897 and 894 cm^{-1} for 3.3 and 1.4 mol% $H_4PMo_{11}VO_{40}/SiO_2$, respectively. This band shift suggests the presence of strong interactions between $H_4PMo_{11}VO_{40}$ and the SiO_2 surface. A model for the interaction between $H_3PW_{12}O_{40}$ and the SiO_2 surface, where the protons of $H_3PW_{12}O_{40}$ react with OH groups on SiO_2 to form $–Si–OH_2^+ \cdots H_2PW_{12}O_{40}^-$, has been proposed on the basis of ^1H NMR studies [44–47]. Similar interactions between $H_4PMo_{11}VO_{40}$ and the SiO_2 surface could be present in the case of $H_4PMo_{11}VO_{40}/SiO_2$. Since the Raman bands were shifted in the case of SiO_2-supported $H_4PMo_{11}VO_{40}$, the Keggin structure was distorted to some degree. For 0.37 mol% $H_4PMo_{11}VO_{40}/SiO_2$, only weak bands were observed, meaning that the peak position could not be determined precisely. However, at least some $H_4PMo_{11}VO_{40}$ still had a Keggin structure.

Fig. 7 shows a BN-TPD profile for 1.4 mol% $H_4PMo_{11}VO_{40}/SiO_2$; here, a mass spectrometer was utilized as the detector. BN adsorbs
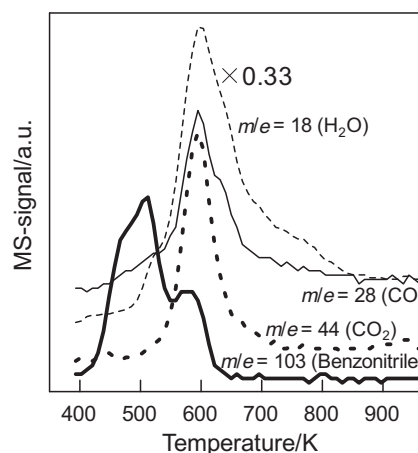

Fig. 7. BN-TPD profiles of 1.4 mol% $H_4PMo_{11}VO_{40}/SiO_2$. A mass spectrometer was utilized as the detector.

only on the outermost surface of a solid heteropolyacid [48], and thus, the number of protons on the outermost surface of heteropolyacid crystallites can be estimated from BN-TPD profiles. However, as shown in Fig. 7, not only BN (m/e = 103) but also H_2O, CO, and CO_2 (m/e = 18, 28, and 44, respectively), which form by the oxidative decomposition of BN with lattice oxygen from $H_4PMo_{11}VO_{40}$, were detected in the effluent gas while measuring the TPD profile. Thus, we estimated the amount of BN adsorbed on the catalyst by taking into account the amount of CO and CO_2. In Fig. 8, the amounts of adsorbed BN per unit catalyst weight are plotted as a function of the loading amount of $H_4PMo_{11}VO_{40}$. The amount of adsorbed BN on the unsupported $H_4PMo_{11}VO_{40}$ was 4.6 µmol g^{-1}. If two molecules of BN are adsorbed on the outermost surface of a molecule of $H_4PMo_{11}VO_{40}$, only 0.4% of $H_4PMo_{11}VO_{40}$ is exposed on the outermost surface of unsupported $H_4PMo_{11}VO_{40}$. In other words, the mean particle size of unsupported $H_4PMo_{11}VO_{40}$ is 1200 nm (1.2 µm). The amounts of adsorbed BN for the supported catalysts were larger than that for the unsupported $H_4PMo_{11}VO_{40}$. 1.4 mol% $H_4PMo_{11}VO_{40}/SiO_2$ adsorbed the largest amount of BN, i.e. 75 µmol g$_{cat}^{-1}$, which is 16 times larger than that adsorbed by unsupported $H_4PMo_{11}VO_{40}$. The amounts of adsorbed BN for 0.37 and 3.3 mol% $H_4PMo_{11}VO_{40}/SiO_2$ are about 10 times larger than that for unsupported $H_4PMo_{11}VO_{40}$. The mean particle sizes of the
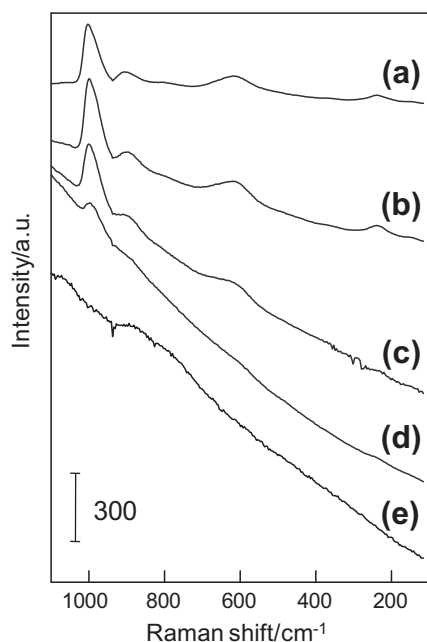

Fig. 6. Raman spectra of unsupported and SiO_2-supported $H_4PMo_{11}VO_{40}$ before the reaction. (a) Unsupported $H_4PMo_{11}VO_{40}$, SiO_2-supported $H_4PMo_{11}VO_{40}$ with (b) 3.3 mol%, (c) 1.4 mol%, (d) 0.37 mol%, and (e) SiO_2.
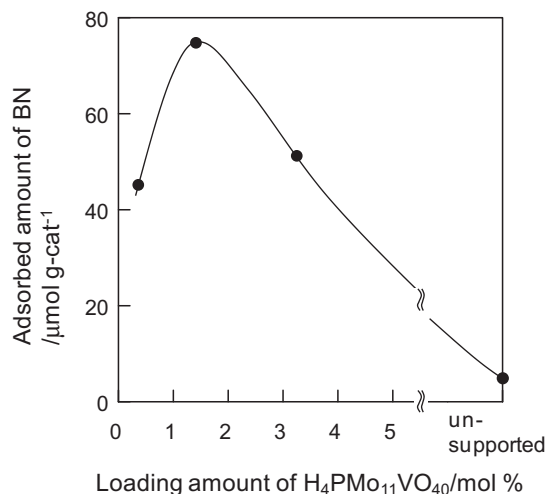

Fig. 8. Adsorbed amount of BN per catalyst weight on unsupported and SiO_2-supported $H_4PMo_{11}VO_{40}$.

supported catalysts were 11, 20, and 48 nm for 0.37, 1.4, and 3.3 mol% $H_4PMo_{11}VO_{40}/SiO_2$, respectively. On the basis of these findings, we concluded that microparticles of $H_4PMo_{11}VO_{40}$ were obtained by supporting $H_4PMo_{11}VO_{40}$ on SiO_2. As a result, the number of $H_4PMo_{11}VO_{40}$ available for the reaction is larger, thus improving the catalytic activity. However, the trend in the catalytic activity shown in Fig. 2 does not fully agree with that in the amounts of adsorbed BN in Fig. 8. For example, the maximum catalytic activity was observed at a loading of 3.3 mol%, whereas the maximum number of $H_4PMo_{11}VO_{40}$ exposed on the outermost surface was observed at a loading of 1.4 mol%. The discrepancy indicates that specific activity per $H_4PMo_{11}VO_{40}$ exposed on the outermost surface is lower for the supported catalysts than it is for the unsupported one. In addition, selectivity of the supported catalysts for the formation of MAA was lower. In order to elucidate the cause, the catalyst after the reaction was investigated.

3.3.2. Post-catalytic oxidation of MAL

Fig. 9 shows XRD patterns for the catalysts after 5 h of reaction. Unsupported $H_4PMo_{11}VO_{40}$ (Fig. 9a) gave a diffraction pattern similar to that before the reaction, although the diffraction lines were less intense and broader. On the other hand, in the case of the supported catalysts (Fig. 9b–d), the diffraction pattern corresponding to $H_4PMo_{11}VO_{40}$ almost disappeared, and sharp diffraction lines attributed to crystalline MoO_3 appeared.

Decomposition of $H_4PMo_{11}VO_{40}$ in the supported catalysts after the reaction was clearer from the Raman spectra. Fig. 10 shows Raman spectra of the catalysts after the reaction. Unsupported $H_4PMo_{11}VO_{40}$ (Fig. 10a) showed bands characteristic of a Keggin structure, and no other bands were detected. Therefore, the Keggin structure of the unsupported $H_4PMo_{11}VO_{40}$ remained intact even after the reaction, although the band intensity decreased. On the other hand, in the case of the supported catalysts (Fig. 10b–d), Raman bands attributed to not only $H_4PMo_{11}VO_{40}$ but also MoO_3 (α-MoO_3: 820 and 660 cm^{-1}; β-MoO_3: 849 and 772 cm^{-1} [43,49]) were detected. These results agree with the XRD measurements
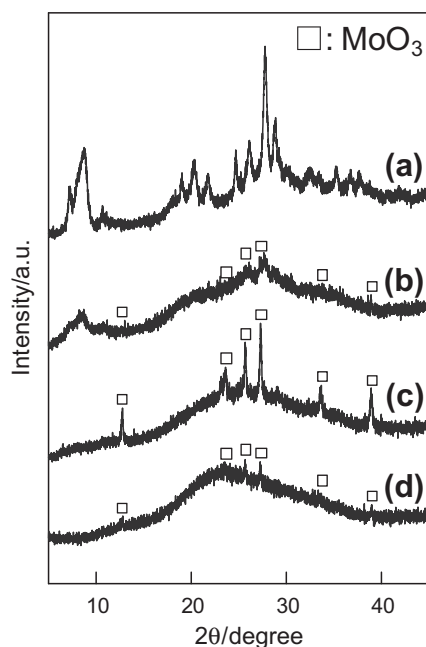

Fig. 9. XRD patterns of unsupported $H_4PMo_{11}VO_{40}$ and SiO_2-supported $H_4PMo_{11}VO_{40}$ after the reaction for 5 h. (a) Unsupported $H_4PMo_{11}VO_{40}$ and SiO_2-supported $H_4PMo_{11}VO_{40}$ with loadings of (b) 3.3 mol%, (c) 1.4 mol%, and (d) 0.37 mol%. Reaction conditions: MAL:O_2:H_2O:N_2 = 3:6:15:76, temperature = 573 K, and total pressure = 0.1 MPa.
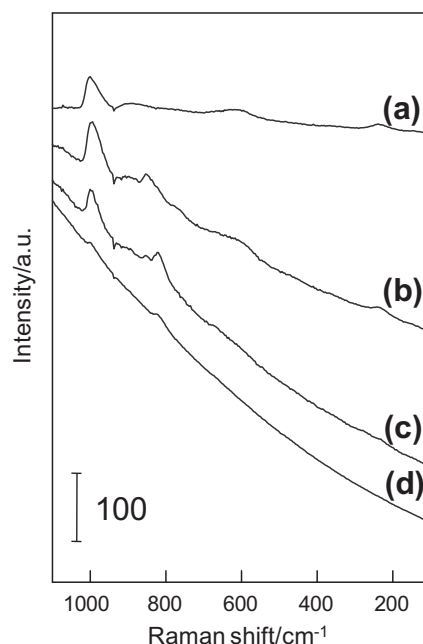
Fig. 10. Raman spectra of unsupported $H_4PMo_{11}VO_{40}$ and SiO_2-supported $H_4PMo_{11}VO_{40}$ after the catalytic reaction for 5 h. (a) Unsupported $H_4PMo_{11}VO_{40}$, and SiO_2-supported $H_4PMo_{11}VO_{40}$ with loadings of (b) 3.3 mol%, (c) 1.4 mol%, and (d) 0.37 mol%. Reaction conditions: MAL:O_2:H_2O:N_2 = 3:6:15:76, temperature = 573 K, and total pressure = 0.1 MPa.

(Fig. 9). In particular, in the spectra of 0.37 mol% $H_4PMo_{11}VO_{40}$/SiO_2 (Fig. 10d), the Raman bands of $H_4PMo_{11}VO_{40}$ were very weak, and a Raman band attributed to α-MoO_3 was observed at 820 cm^{-1}. Broad Raman bands at around 900 cm^{-1} for the supported catalysts were attributable to Mo–V mixed oxide [50], but the intensities were weak. Therefore, we concluded that most of the $H_4PMo_{11}VO_{40}$ on 0.37 mol% $H_4PMo_{11}VO_{40}/SiO_2$ decomposed mainly to MoO_3 during the reaction. Destabilization of heteropolyacids after supporting them on SiO_2 has been reported for $H_3PMo_{12}O_{40}/SiO_2$ [51] and for $H_5PMo_{11}V_2O_{40}/SiO_2$ [41]. Our results are consistent with previously reported ones.

### 3.4. Catalytic oxidation of MAL over MoO_3/SiO_2 and unsupported MoO_3

As mentioned in Section 3.3, $H_4PMo_{11}VO_{40}$ in the supported catalysts decomposed during the reaction to form mainly MoO_3. The formation of MoO_3 could cause the decrease in activity per $H_4PMo_{11}VO_{40}$ exposed on the outermost surface and in selectivity for the formation of MAA. Therefore, we prepared 3.96 mol% MoO_3/SiO_2 and examined its catalytic performance for the oxidation of MAL. The loading amount of MoO_3 (3.96 mol%) corresponded to the amount of molybdenum present in 0.37 mol% $H_4PMo_{11}VO_{40}$/SiO_2. Catalytic performance of unsupported MoO_3 was also evaluated. Catalytic results are summarized in Table 2 together with those of 0.37 mol% $H_4PMo_{11}VO_{40}/SiO_2$ and unsupported $H_4PMo_{11}VO_{40}$. The catalytic activity of 3.96 mol% MoO_3/SiO_2 was 7 µmol g^{-1} min^{-1}, and the selectivity for the formation of MAA was only 18%. In addition, unsupported MoO_3 also showed low activity and comparable selectivity for MAA to 0.37 mol% $H_4PMo_{11}VO_{40}/SiO_2$. These are much lower than those for unsupported $H_4PMo_{11}VO_{40}$. Therefore, it was concluded that the formation of MoO_3 caused the decrease in the catalytic performance of the supported catalysts, especially of the catalysts with low loadings.

The reaction mechanism for the oxidation of MAL to MAA over unsupported $H_3PMo_{12}O_{40}$ is proposed as Scheme 2, where the first step reaction is promoted by Brønsted acid sites and then

Table 2
Catalytic performance of 3.96 mol% MoO_3/SiO_2, unsupported MoO_3, 0.37 mol% $H_4PMo_{11}VO_{40}/SiO_2$, and unsupported $H_4PMo_{11}VO_{40}$ for the oxidation of MAL.

Catalyst	Activity (μmol h^{-1} g$^{-1}_{cat}$)	Selectivity (%)				(Conv.) (%)
		MAA	AcOH	CO_x	Others[a]	
3.96 mol% MoO_3/SiO_2	7	18	25	47	10	(7)
MoO_3	7	41	6	53	n.d.[b]	(5)
0.37 mol% $H_4PMo_{11}VO_{40}/SiO_2$	15	43	11	36	10	(8)
$H_4PMo_{11}VO_{40}$	13	75	5	16	4	(8)

[a] Others were acetone, acetaldehyde, acrolein, and acrylic acid.
[b] Others was not detected with a gas chromatograph.
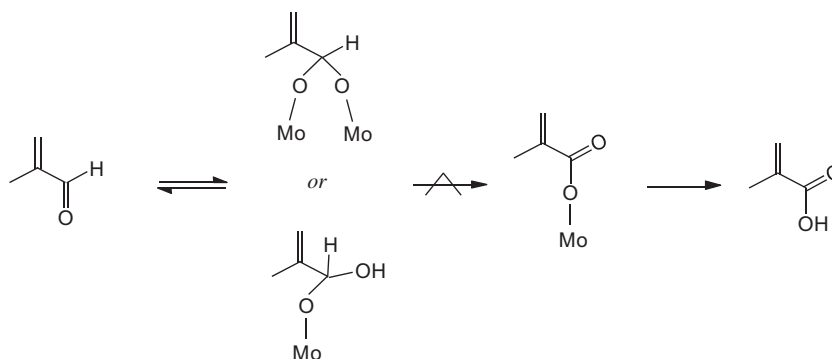
Scheme 2. Proposed reaction mechanism for the oxidation of MAL over unsupported $H_3PMo_{12}O_{40}$ [11,14,52].

the intermediates having C–O–Mo bonds are oxidized with the lattice oxygen (Mars and van Krevelen mechanism) to form MAA [11,14,52]. Thus, acid sites are indispensable for the selective formation of MAA. MoO_3 possesses acid sites, but they are weak [53]. Therefore, the first step reaction may not be promoted and consequently, the selective oxidation forming MAA was inhibited over MoO_3/SiO_2 and unsupported MoO_3.

3.5. Decomposition process of $H_4PMo_{11}VO_{40}$ on SiO_2

During the course of the catalyst preparation, the catalysts were calcined at 523 K and were then pretreated at a higher temperature of 593 K before the reaction. On the basis of the time courses of the reaction shown in Fig. 1, changes in the conversion and selectivity were not so large as a function of time. Thus, it is reasonable that the structure of the catalysts do not change drastically during the catalytic reaction.

We investigated the decomposition process of $H_4PMo_{11}VO_{40}$ under the pretreatment conditions. It is well known that heteropolyacids undergo decomposition with deprotonation during thermal treatment [46]. Fig. 11 shows XRD patterns of the catalysts obtained after thermal treatment at 573 K for 5 h in a gas flow composed of O_2, H_2O, and N_2, that is, under conditions the same as the pretreatment conditions. Unsupported $H_4PMo_{11}VO_{40}$ gave broad diffraction lines (Fig. 11a) compared with fresh catalyst (Fig. 4a), and the XRD pattern was similar to that after the reaction (Fig. 8a). On the other hand, 0.37 mol% $H_4PMo_{11}VO_{40}/SiO_2$ after treatment showed sharp diffraction lines corresponding to MoO_3 (Fig. 12b). This XRD pattern is similar to that after the catalytic reaction (Fig. 8d). The similarity indicates that the Keggin structure of $H_4PMo_{11}VO_{40}$ decomposes to form MoO_3 in the pretreatment stage.

Fig. 12 shows XRD patterns of the 1.4 mol% $H_4PMo_{11}VO_{40}/SiO_2$ after the catalytic oxidation for 5 h in the temperature range of 523–563 K, which is lower than the normal reaction temperature (573 K). In the pattern after the reaction at 523 K (Fig. 12c), diffraction lines corresponding to $H_4PMo_{11}VO_{40}$ were observed. However, in the pattern at 553 K (Fig. 12b), diffraction lines were barely
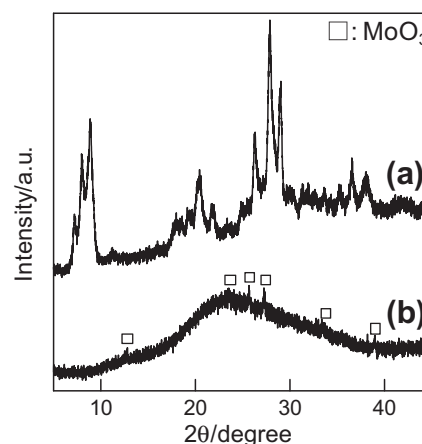
Fig. 11. XRD patterns of (a) unsupported $H_4PMo_{11}VO_{40}$ and (b) 0.37 mol% $H_4PMo_{11}VO_{40}/SiO_2$ after thermal treatment for 5 h. Conditions of thermal treatment: O_2:H_2O:N_2 = 6:15:76, temperature = 573 K, and total pressure = 0.1 MPa.

visible. Furthermore, in the pattern at 563 K, diffraction lines corresponding to MoO_3 appeared. The Raman spectra of these samples are consistent with the XRD patterns (data not shown).

Mestl et al. have revealed by using Raman technique the structural transformation of unsupported $H_4PMo_{11}VO_{40}$ induced by thermal treatment as follows [54,55]: vanadyl and molybdenyl species are expelled from the Keggin cage and defective Keggin structures are formed. These defective structures further disintegrate to Mo_3O_{13} triads, which finally oligomerize to form crystalline MoO_3. On the SiO_2 support, the similar transformation may take place. As discussed previously, the decomposition temperature of $H_4PMo_{11}VO_{40}$ decreased after it was supported on SiO_2. As mentioned in Section 3.3.1, the protons of $H_4PMo_{11}VO_{40}$ interact with SiO_2, i.e., $-SiOH_2^+ \cdots H_3PMo_{11}VO_{40}$. This may result in the changes in the structure of $H_4PMo_{11}VO_{40}$, lowering the thermal stability of $H_4PMo_{11}VO_{40}$. Thus, $H_4PMo_{11}VO_{40}$ decomposed at lower temperatures.

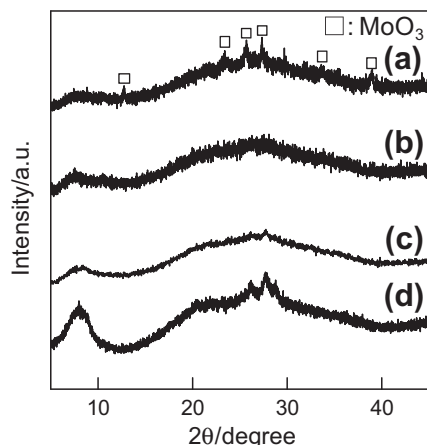**Fig. 12.** XRD patterns of 1.4 mol% $H_4PMo_{11}VO_{40}/SiO_2$ after the reaction for 5 h at (a) 563 K, (b) 553 K, and (c) 523 K. Reaction conditions: $MAL:O_2:H_2O:N_2 = 3:6:15:76$, temperature = 573 K, and total pressure = 0.1 MPa, and $WF^{-1} = 23$ g_{-cat} h mol^{-1}_{-MAL}.

4. Conclusions

Catalytic activity per unit catalyst weight for the oxidation of MAL significantly increased by supporting $H_4PMo_{11}VO_{40}$ on SiO_2 due to the high dispersion of $H_4PMo_{11}VO_{40}$ on SiO_2. In particular, 3.3 mol% $H_4PMo_{11}VO_{40}/SiO_2$ had an activity that was five-times higher than that of unsupported $H_4PMo_{11}VO_{40}$ and a selectivity for the formation of MAA comparable to that of the unsupported catalyst. However, the supported catalysts with low $H_4PMo_{11}VO_{40}$ loadings (0.37 mol%) showed only low selectivities for MAA formation. In the case of the SiO_2-supported catalysts, $H_4PMo_{11}VO_{40}$ decomposed at a lower temperature, and almost all of the $H_4PMo_{11}VO_{40}$ decomposed during pretreatment conducted at 573 K before the catalytic reaction. The decomposition of $H_4PMo_{11}VO_{40}$ results in a decrease in the catalytic performances of the supported catalysts with low loadings.

References

[1] M. Wada, Petrotech 15 (1992) 452.
[2] M. Misono, N. Nojiri, Appl. Catal. A 64 (1990) 1.
[3] N. Shimizu, Petrotech 6 (1983) 778.
[4] J.B. Black, N.J. Claydon, P.L. Gai, J.D. Scott, E.M. Serwicke, J.B. Goodenough, J. Catal. 106 (1987) 1.
[5] S. Tatematsu, T. Hibi, T. Okukara, M. Misono, Chem. Lett. (1987) 865.
[6] N. Mizuno, M. Misono, Chem. Lett. (1987) 967.
[7] Japan Patent 1975-23013, Mitsubishi Rayon.
[8] L. Marosi, G. Cox, A. Tenten, H. Hibst, J. Catal. 194 (2000) 140.
[9] Japan Patent 1992-63139, Sumitomo Chemical.
[10] T. Komaya, M. Misono, Chem. Lett. (1983) 1177.
[11] Y. Konishi, K. Sakata, M. Misono, Y. Yoneda, J. Catal. 77 (1982) 169.
[12] V. Ernst, Y. Barbaux, P. Courtine, Catal. Today 1 (1987) 167.
[13] L.M. Deußer, J.W. Gaube, F.G. Martin, H. Hibst, Stud. Surf. Sci. Catal. 101 (1996) 981.
[14] N. Mizuno, T. Watanabe, M. Misono, Bull. Chem. Soc. Jpn. 64 (1991) 243.
[15] Y. Yamamoto, S. Hatanaka, K. Tsuji, K. Tsuneyama, R. Ohnishi, H. Imai, Y. Kamiya, T. Okuhara, Appl. Catal. A 55 (2008) 344.
[16] J. Zhang, R. Ohnishi, T. Okuhara, Y. Kamiya, Appl. Catal. A 68 (2009) 353.
[17] J. Zhang, R. Ohnishi, T. Okuhara, Y. Kamiya, J. Catal. 254 (2008) 263.
[18] T. Okuhara, N. Mizuno, M. Misono, Adv. Catal. 41 (1996) 113.
[19] H. Li, H. Yin, T. Jiang, T. Hu, J. Wu, Y. Wada, Catal. Commun. 7 (2006) 778.
[20] Y. Izumi, M. Urabe, A. Onaka, Zeolite, Clay and Heteropoly Acid in Organic Reactions, VCH, Weinheim, 1992.
[21] H. Liu, E. Iglesia, J. Phys. Chem. B 107 (2003) 10840.
[22] K. Brückman, M. Che, J. Haber, J.M. Tatibouet, Catal. Lett. 25 (1994) 225.
[23] S. Damyanova, M.L. Cubeiro, J.L.F. Fierro, J. Mol. Catal. A 142 (1999) 85.
[24] L.M. Gomez Sainero, S. Damyanova, J.L.G. Fierro, Appl. Catal. A 208 (2001) 63.
[25] H. Kim, J.C. Jung, P. Kim, S.H. Yeom, K.-Y. Lee, I.K. Song, J. Mol. Catal. A 259 (2006) 150.
[26] A.A. Spojakina, N.G. Kostova, B. Sow, M.W. Stamenova, K. Jiratova, Catal. Today 65 (2001) 315.
[27] K. Nowińska, M. Sopa, D. Szuba, Catal. Lett. 39 (1996) 275.
[28] Y. Liu, K. Murata, M. Inaba, N. Mimura, Catal. Commun. 4 (2003) 281.
[29] M. Sopa, A. Wącław-Held, M. Grossy, J. Pijanka, K. Nowińska, Appl. Catal. A 285 (2005) 119.
[30] S. Gao, J.B. Moffat, Appl. Catal. A 229 (2002) 245.
[31] N. Lingaiah, K.M. Reddy, P. Nagaraju, P.S. Prasad, I.E. Wachs, J. Phys. Chem. C 112 (2008) 8294.
[32] R.D. Gall, C.L. Hill, J.E. Walker, J. Catal. 159 (1996) 473.
[33] R.D. Gall, C.L. Hill, J.E. Walker, Chem. Mater. 8 (1996) 2523.
[34] Z. Karimi, A.R. Mahjoub, F.D. Aghdam, Inorg. Chim. Acta 362 (2009) 3725.
[35] K.T. Venkateswara Rao, P.S.N. Rao, P. Nagaraju, P.S. Sai Prasad, N. Lingaiah, J. Mol. Catal. A 303 (2009) 84.
[36] Z. Weng, J. Wang, S. Zhang, C. Yan, X. Jian, Catal. Commun. 10 (2008) 125.
[37] P. Sharma, A. Patel, Appl. Surf. Sci. 255 (2009) 7635.
[38] P. Sharma, A. Patel, J. Mol. Catal. A 299 (2009) 37.
[39] H. Kim, J.C. Jung, D.R. Park, S.-H. Baeck, I.K. Song, Appl. Catal. A 159 (2007) 320.
[40] H. Kim, J.C. Jung, S.H. Yeom, K.-Y. Lee, I.K. Song, J. Mol. Catal. A 21 (2006) 248.
[41] K. Brückman, M. Che, J. Haber, J.N. Tatibouet, Catal. Lett. 251 (1995) 225.
[42] T. Ilkenhans, B. Herzog, T. Braun, R. Schlögl, J. Catal. 275 (1995) 153.
[43] A. Predoeva, S. Damyanova, E.M. Gaigneaux, L. Petrov, Appl. Catal. A 14 (2007) 319.
[44] V.M. Mastikhin, S.M. Kulikov, A.V. Nosov, I.V. Kozhevnikov, I.L. Mudrakovsky, M.N. Timofeeva, J. Mol. Catal. 60 (1995) 65.
[45] F. Lefebvre, J. Chem. Soc., Chem. Commun. (1992) 756.
[46] N. Legagneux, J.-M. Basset, A. Thomas, F. Lefebvre, Al. Goguet, J. Sá, C. Hardacre, Dalton Trans. (2009) 2235.
[47] A.D. Newman, D.R. Brown, P. Siril, A.F. Lee, K. Wilson, Phys. Chem. Chem. Phys. 8 (2006) 2893.
[48] T. Sugii, R. Ohnishi, J. Zhang, A. Miyaji, Y. Kamiya, T. Okuhara, Catal. Today 116 (2006) 179.
[49] E. Haro-Poniatowski, M. Jouanne, J.F. Morhange, C. Julien, R. Diamant, M. Fernández-Guasti, G.A. Fuentes, J.C. Alonso, Appl. Surf. Sci. 674 (1998) 127.
[50] M. Olga Guerrero-Pérez, Jamal N. Al-Saeedi, Vadim V. Guliants, Miguel A. Bañares, Appl. Catal. A 260 (2004) 93.
[51] C. Rocchiccioli-Deltcheff, A. Aouissi, S. Launay, M. Fournier, J. Mol. Catal. A 114 (1996) 331.
[52] M. Misono, K. Sakata, Y. Yoneda, in: T. Seiyama, K. Tanabe (Eds.), Proc. 7th Int. Congr. Catal., Tokyo, 1980, Kodansha/Elsevier, Tokyo/Amsterdam, 1981, p. 1047.
[53] K. Tanabe, Solid Acid and Bases, Their Catalytic Properties, Kodansha/Academic Press, Tokyo/New York, 1970, p. 57.
[54] G. Mestl, T. Ilkenhans, D. Spielbauer, M. Dieterle, O. Timpe, J. Kröhnert, F. Jentoft, H. Knözinger, R. Schlögl, Appl. Catal. A 210 (2001) 13.
[55] J. Melsheimer, J. Kröhnert, R. Ahmad, S. Klokishner, F.C. Jentoft, G. Mestl, R. Schlögel, Phys. Chem. Chem. Phys. 4 (2002) 2398.